
PERGAMON

Journal of the Mechanics and Physics of Solids
50 (2002) 979–1009

JOURNAL OF THE
MECHANICS AND
PHYSICS OF SOLIDS

www.elsevier.com/locate/jmps

Dramatically stiffer elastic composite materials due to a negative stiffness phase?

R.S. Lakes[a,b,*], W.J. Drugan[a]

[a] *Department of Engineering Physics, Engineering Mechanics Program, Materials Science Program, 1500 Engineering Drive, University of Wisconsin, Madison, WI 53706, USA*
[b] *Rheology Research Center, 1500 Engineering Drive, University of Wisconsin, Madison, WI 53706, USA*

Received 20 February 2001; accepted 7 September 2001

Abstract

Composite materials of extremely high stiffness can be produced by employing one phase of negative stiffness. Negative stiffness entails a reversal of the usual codirectional relationship between force and displacement in deformed objects. Negative stiffness structures and materials are possible, but unstable by themselves. We argue here that composites made with a small volume fraction of negative stiffness inclusions can be stable and can have overall stiffness far higher than that of either constituent. This high composite stiffness is demonstrated via several exact solutions within linearized and also fully nonlinear elasticity, and via the overall modulus tensor estimate of a variational principle valid in this case. We provide an initial discussion of stability, and adduce experimental results which show extreme composite behavior in selected viscoelastic systems under sub-resonant sinusoidal load. Viscoelasticity is known to expand the space of stability in some cases. We have not yet proved that purely elastic composite materials of the types proposed and analyzed in this paper will be stable under static load. The concept of negative stiffness inclusions is buttressed by recent experimental studies illustrating related phenomena within the elasticity and viscoelasticity contexts.

Keywords: Elastic material; Particle reinforced material; Phase transformation; Ferroelectric material; Composite material

1. Introduction

How stiff can a composite be? In contrast to homogeneous materials, composite materials have heterogeneous structures upon which the overall material properties depend.

* Corresponding author. Fax: +1-608-263-7451.
E-mail address: lakes@engr.wisc.edu (R.S. Lakes).

0022-5096/02/$ - see front matter
PII: S0022-5096(01)00116-8

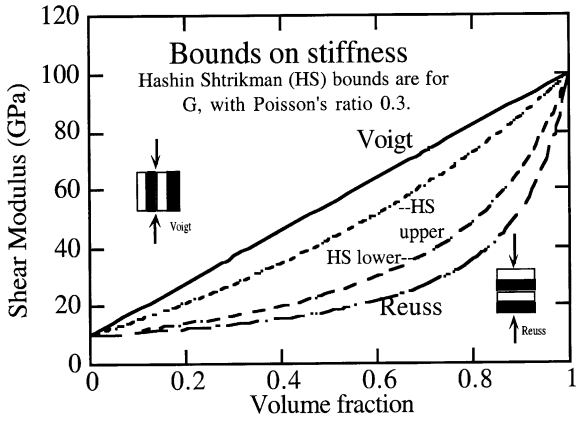

Fig. 1. Modulus (stiffness) vs. volume fraction of the stiffer constituent for several elastic composites. HS refers to the Hashin–Shtrikman bounds for isotropic composites. The Voigt and Reuss structures (inset) are anisotropic (direction dependent). The stiff phase has a stiffness of 100 GPa, the soft phase, 10 GPa.

For an elastic two-phase composite, comprised of isotropic phases, the stiffnesses of Voigt and Reuss composites described below represent rigorous upper and lower bounds (Paul, 1960) on the Young's modulus for a given volume fraction of one phase (Fig. 1). The Hashin–Shtrikman (1963) equations represent rigorous upper and lower bounds on the elastic stiffness of macroscopically *isotropic* composites. These bounds are tighter than the Voigt and Reuss bounds. The structure that attains the Voigt bound (Fig. 1) is aligned in the direction of the load so that each phase experiences the same strain. The model is one-dimensional, so the Poisson effects in compression are neglected; alternatively, one may consider shear deformation. The Voigt upper bound formula, also called the rule of mixtures, is

$$E_c = E_1 V_1 + E_2 V_2, \tag{1.1}$$

in which E_c, E_1 and E_2 refer to the Young's modulus (stiffness) of the composite, phases 1 and 2, and V_1 and V_2 refer to the volume fraction of phases 1 and 2 with $V_1 + V_2 = 1$. The structure that attains the Reuss bound (Fig. 1) is aligned perpendicular to the direction of the load so that each phase experiences the same stress. The Reuss lower bound formula is

$$\frac{1}{E_c} = \frac{V_1}{E_1} + \frac{V_2}{E_2}. \tag{1.2}$$

The bounding theorems state that no composite can be stiffer than the Voigt bound (Paul, 1960) and no macroscopically isotropic composite can be stiffer than the Hashin–Shtrikman (Hashin, 1962; Hashin and Shtrikman, 1963) upper bound. However, positive definiteness of the strain energy density was assumed in proving these theorems. Moreover, based on the Voigt upper bound relation and the corresponding upper curve in Fig. 1, it would seem that no composite could be stiffer than the stiffest constituent. That is true if each phase has a positive stiffness.

The purpose of this paper is to explore the effects of constituents of negative stiffness in composite materials. It is shown that if one phase has the appropriate negative stiffness, the overall stiffness of the composite can be made dramatically large. It is also shown that in the presence of a small nonlinearity, extremely high stiffness can be achieved without singularity of the elastic fields. We remark that small viscoelastic damping also ameliorates singularities in the strain. Methods of achieving negative stiffness are presented. The question of stability of materials and composites is examined in a preliminary manner, by summarizing what is known and discussing how it applies in the present context. Further investigation of the stability of such composite materials under various load situations is needed, and is under way. Finally, the relation between experimental realization of these concepts and the present analysis is discussed.

2. Composite cells and materials with a negative stiffness phase

2.1. Lumped one-dimensional model

We consider the effect of phases of negative stiffness in several composite microstructures. For the Voigt structure, governed by Eq. (1.1), a phase of negative stiffness simply reduces the overall composite stiffness, as one might expect.

The situation is different in a Reuss composite (Fig. 1 inset). For purposes of visualization, write the Reuss equation (1.2) for the composite stiffness in terms of the compliance $J = 1/E$ rather than the stiffness E:

$$J_c = J_1 V_1 + J_2 V_2. \tag{2.1}$$

Suppose that one phase has a negative stiffness, hence a negative compliance. This compliance may be added to a positive compliance of similar magnitude to obtain a compliance which is very small, tending to zero. The corresponding composite stiffness is then very large, tending to infinity (Fig. 2). Large stiffness values arise in the structure when the positive and negative stiffness phases are nearly balanced because the interface between the constituents moves much more than the applied load, giving rise to large strain energy in each phase. This is illustrated later via an explicit elasticity solution. As we shall see in Section 4, the Reuss model containing one element of each phase is stable only when constrained. Moreover, negative stiffness of large magnitude is possible in a constrained system; however, the region for which Reuss composite stiffness tends to positive infinity is unstable.

2.2. Stress around a spherical inclusion in uniaxial tension

The elastic solution (Goodier, 1933) for a single spherical inclusion provides an understanding of the physical basis for effects of inclusions of negative stiffness. Consider a spherical elastic inclusion in an elastic matrix, under tension. The inclusion elongates the least for a stiff inclusion. It elongates more for an "inclusion" identical to the matrix G_m, more for a cavity of zero stiffness, and yet more for an inclusion of negative stiffness G_i. The deformation within and near the inclusion approaches infinity as G_i

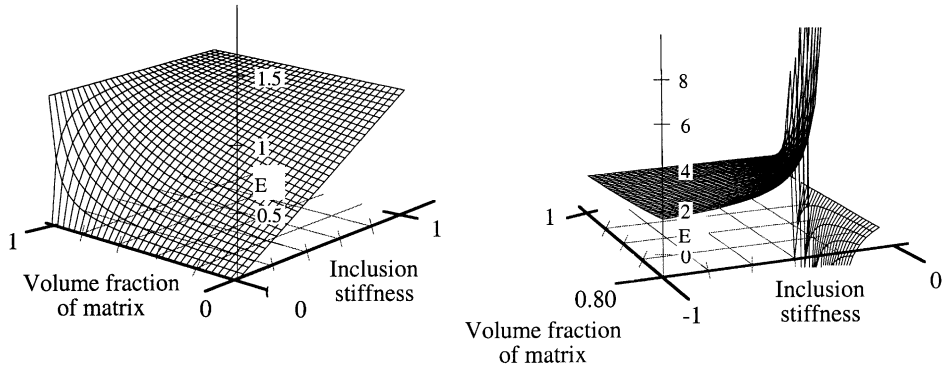

Fig. 2. Calculated composite stiffness E vs. volume fraction and "inclusion" stiffness (normalized to "matrix" stiffness) for a Reuss composite structure. One constituent can have negative stiffness and one constituent has a positive stiffness of $+1$, in arbitrary units of stiffness. Diagram is based on Eq. (1.2). Composite stiffness can substantially exceed the stiffness of either phase. Left, positive inclusion stiffness; right, negative inclusion stiffness.

tends to $-1.1G_m$ (for a Poisson's ratio of 0.3 and small volume fraction). Consider an inclusion which has a negative shear modulus of smaller magnitude than the positive modulus of the matrix. The inclusion is effectively under displacement constraint, hence stabilized. As the negative inclusion stiffness approaches the matrix stiffness in magnitude, the deformation at its surface becomes much greater than the overall asymptotic deformation of the composite. Since local strain becomes much larger than applied strain in an elastic composite of this type, a relatively large energy is stored in a small overall deformation, corresponding to a composite stiffness of large magnitude.

2.3. An explicit model problem: sphere containing a spherical inclusion

Here we illustrate explicitly precisely what happens to a full, exact elasticity solution when one phase of a composite has a sufficiently negative stiffness. We analyze a spherically symmetric problem consisting of a spherical matrix of one isotropic material containing a spherical inclusion of another, when the boundary conditions are spherically symmetric. The problem will be analyzed first within linearized elasticity theory, and to verify that the conclusions obtained are not artifacts of the infinitesimal-displacement-gradient formulation, the problem will be analyzed again within a fully nonlinear finite deformation formulation. The linear version of this problem was treated by Hill (1963). The analysis presented here shows that assumptions regarding the sign of the constituent moduli are not needed. We recognize that the problem analyzed here is not a "representative volume element" for a matrix–inclusion composite when the inclusions have negative stiffness. However, this problem displays very similar features to the results presented for composite materials in the next sections (Sections 2.4 and 2.5), and it permits a detailed exploration of how negative inclusion stiffness affects the stress, strain and displacement fields.

2.3.1. Solutions within linearized elasticity theory

Consider a sphere of Material 2, having radius b and elastic bulk and shear moduli B_2, G_2, containing a concentric spherical inclusion of Material 1, having radius a and moduli B_1, G_1. We will analyze two problems, both having spherically symmetric boundary conditions. The analysis of these problems is straightforward, but we summarize it here because the explicit solutions obtained are highly informative and comparisons with the ensuing finite deformation solutions are valuable.

For spherically symmetric equilibrium problems, the general three-dimensional equations of homogeneous, isotropic linearized elasticity have the following general solution for the nonzero components of the stress and infinitesimal strain tensors $\boldsymbol{\sigma}, \boldsymbol{\varepsilon}$ and the displacement vector $\mathbf{u}$, in terms of spherical coordinates r, θ, ϕ:

$$u_r = \alpha r + \frac{\beta}{r^2}, \tag{2.2}$$

$$\varepsilon_{rr} = \alpha - 2\frac{\beta}{r^3}, \quad \varepsilon_{\theta\theta} = \varepsilon_{\phi\phi} = \alpha + \frac{\beta}{r^3}, \tag{2.3}$$

$$\sigma_{rr} = 3B\alpha - \frac{4G\beta}{r^3}, \quad \sigma_{\theta\theta} = \sigma_{\phi\phi} = 3B\alpha + \frac{2G\beta}{r^3}, \tag{2.4}$$

where α and β are initially undetermined constants. These solutions apply inside the spherical inclusion, and in the spherical matrix, with appropriate values of the elastic moduli, and with different values, in general, of the constants α, β.

As shown in Appendix A, the effective bulk modulus, i.e., the bulk modulus for the composite sphere, $\bar{B}$, is therefore (where the subscripts 1, 2 indicate inclusion and matrix, respectively)

$$\bar{B} = \frac{b^3 B_2 \alpha_2 - 4G_2\beta_2/3}{\alpha_2 b^3 + \beta_2}. \tag{2.5}$$

Problem 1: *prescribed uniform radial stress.* First, we consider application of a uniform radial stress of magnitude σ on the outer boundary of the spherical matrix, giving the boundary condition $\sigma_{rr}(b) = \sigma$. The other conditions to be applied are the requirement of zero displacement at the center of the spherical inclusion, $u_r(0) = 0$, and continuity of σ_{rr} and u_r across the inclusion/matrix boundary $r = a$. These conditions give four equations for the four unknown constants (α, β in each material, again employing subscripts 1, 2 to indicate inclusion and matrix, respectively). The solution is

$$\alpha_1 = \frac{(3B_2 + 4G_2)b^3\sigma}{\gamma}, \quad \beta_1 = 0,$$

$$\alpha_2 = \frac{(3B_1 + 4G_2)b^3\sigma}{\gamma}, \quad \beta_2 = -\frac{3(B_1 - B_2)a^3 b^3 \sigma}{\gamma}, \tag{2.6}$$

where

$$\gamma = 12a^3 G_2(B_1 - B_2) + 3b^3 B_2(3B_1 + 4G_2)$$

$$= 9b^3 B_2 \left\{ \left[V_1 \frac{2(1-2\nu_2)}{1+\nu_2} + 1 \right] B_1 + \frac{2(1-2\nu_2)}{1+\nu_2}(1 - V_1)B_2 \right\}. \tag{2.7}$$

Here, we employed the relation $2G = 3B(1-2\nu)/(1+\nu)$, where ν is Poisson's ratio, and the fact that the volume fraction of the inclusion is given by $V_1 = a^3/b^3$. Now, we employ Eq. (2.6) to find that the composite bulk modulus Eq. (2.5) becomes

$$\bar{B} = \frac{B_2(3B_1 + 4G_2) + 4V_1G_2(B_1 - B_2)}{3B_1 + 4G_2 - 3V_1(B_1 - B_2)}$$
$$= \frac{B_1(1+2V_1) + 2B_2(1-V_1)(1-2\nu_2)/(1+\nu_2)}{(1-V_1)B_1/B_2 + 2(1-2\nu_2)/(1+\nu_2) + V_1}. \tag{2.8}$$

This shows that *the composite sphere bulk modulus becomes infinite when the inclusion bulk modulus attains the* (*negative*) *value*:

$$B_1 = -\frac{1}{1-V_1}\left[\frac{2(1-2\nu_2)}{1+\nu_2} + V_1\right]B_2. \tag{2.9}$$

Eq. (2.8) also shows that the singularity in the composite bulk modulus changes sign as the ratio of constituent moduli traverses its critical value.

Note that Eq. (2.7) becomes zero when

$$B_1 = -\frac{2(1-V_1)(1-2\nu_2)}{2V_1(1-2\nu_2)}B_2. \tag{2.10}$$

When the inclusion volume fraction is very small ($V_1 \to 0$) and for $\nu_2 = 0.3$, observe that both Eqs. (2.9) and (2.10) reduce to $B_1 = -0.615B_2$. The criteria for singular composite bulk modulus and for singular elastic fields become different for nonzero inclusion concentration. In particular, as B_1 decreases from zero, Eqs. (2.9) and (2.10) show that $\gamma = 0$ is attained before $\bar{B}$ becomes infinite, for all nonzero inclusion concentrations. This can be seen from the ratio of B_1 of Eq. (2.10) to that of Eq. (2.9), which is always $\leqslant 1$ (the equality occurring when $V_1 \to 0$):

$$\frac{B_1(2.10)}{B_1(2.9)} = \frac{K(1-V_1)^2}{K + V_1(1 + K^2 + KV_1)}, \quad \text{where } K = \frac{2(1-2\nu_2)}{1+\nu_2}. \tag{2.11}$$

This fact is also illustrated in Fig. 3, which plots B_1/B_2 for $\nu_2 = 0.3$, as a function of volume concentration. As Eqs. (2.2)–(2.4) with Eqs. (2.6) and (2.7) show, when $\gamma \to 0$, the stress, strain and displacement fields become infinite *everywhere in the composite* (according to linearized elasticity theory, about which more later).

Problem 2: *prescribed uniform radial displacement*. The second problem we consider involves application of a uniform radial displacement of magnitude u on the outer boundary of the spherical matrix, giving the boundary condition $u_r(b) = u$. The other three conditions enforced are identical to those in Problem 1, to give four equations for the four unknown constants (α, β in each material). The solution is

$$\alpha_1 = \frac{(3B_2 + 4G_2)b^2u}{\delta}, \quad \beta_1 = 0,$$
$$\alpha_2 = \frac{(3B_1 + 4G_2)b^2u}{\delta}, \quad \beta_2 = -\frac{3(B_1 - B_2)a^3b^2u}{\delta}, \tag{2.12}$$

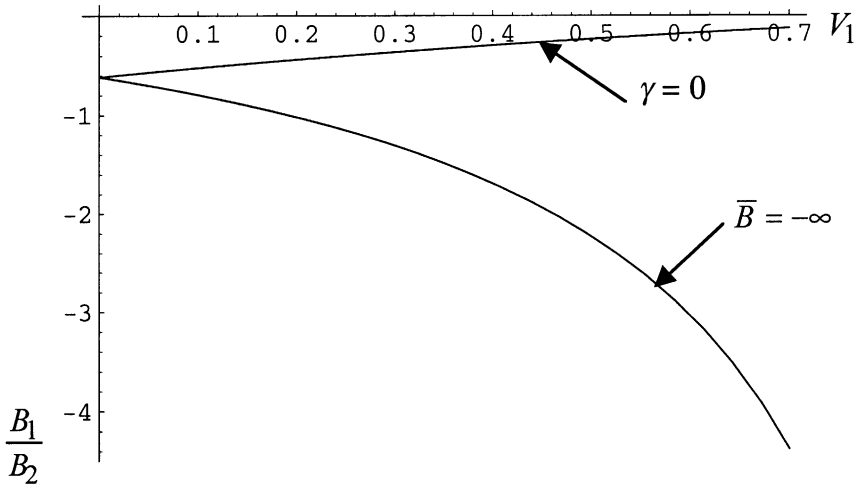

Fig. 3. The bulk modulus ratio B_1/B_2 at which γ of Eq. (2.7) vanishes and at which the effective bulk modulus becomes infinite, as functions of inclusion volume fraction V_1.

where

$$\delta = -3a^3(B_1 - B_2) + b^3(3B_1 + 4G_2). \tag{2.13}$$

Thus, employing Eq. (2.5) with Eqs. (2.12) and (2.13), we confirm for this problem that the composite bulk modulus is still given by Eq. (2.8), and this becomes infinite when the inclusion bulk modulus attains the (negative) value given in Eq. (2.9).

To explore when δ becomes zero, we again employ the relation $2G = 3B(1-2v)/(1+v)$ to rewrite Eq. (2.13) as

$$\delta = -3a^3(B_1 - B_2) + b^3[3B_1 + 6B_2(1-2v_2)]/(1+v_2). \tag{2.14}$$

This shows that δ becomes zero when

$$B_1 = -\frac{1}{1-V_1}\left[2\frac{1-2v_2}{1+v_2} + V_1\right]B_2. \tag{2.15}$$

Observe that this is identical to the value of B_1 that causes the composite bulk modulus to become infinite, as given in Eq. (2.9). This shows, perhaps not surprisingly, that in the inherently more stable displacement-controlled boundary-value problem, extremely large values of the effective bulk modulus can be attained without causing the elastic solution fields obtained to become singular.

To get a feel of the effects under discussion, let us examine a specific example case: a composite having $V_1 = 0.01, v_2 = 0.2$. In this case, Eq. (2.9) shows that the composite bulk modulus becomes (negatively) infinite when the inclusion bulk modulus reaches the value $B_1 = -1.0202B_2$. Let us choose $B_1 = -1.0165B_2$; then Eq. (2.8) shows that $\bar{B} = -10B_2$. For these parameter values, for the case of an imposed displacement, the solutions obtained above for the displacement and strain fields in the composite are plotted in Fig. 4. These illustrate explicitly the qualitative comment

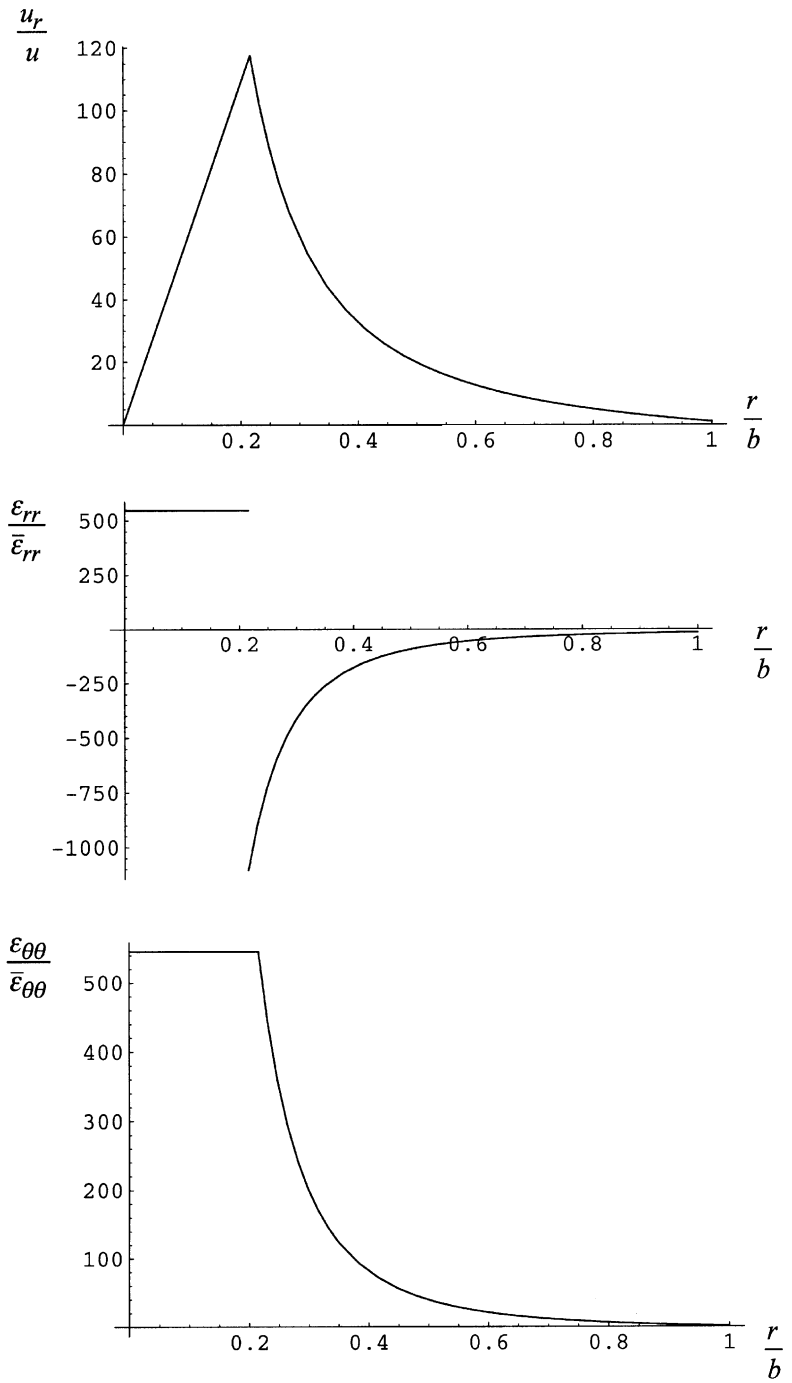

Fig. 4. Displacement and strain fields throughout the spherical composite for the case of an imposed radial displacement u on the outer boundary, for parameter values $V_1 = 0.01, v_2 = 0.2, B_1 = -1.0165B_2$, for which $\bar{B} = -10B_2$.

made earlier that the displacements are very large in the vicinity of the inclusion/matrix interface, and that the strains are very large in the inclusion and in the matrix near the inclusion.

We have just shown that for the displacement-controlled boundary-value problem, one can obtain extremely large *negative* values of the composite bulk modulus, by suitable (negative) choices of the inclusion modulus B_1, and that the linear elastic solution is well behaved as B_1 decreases to such levels. However, for practical applications, one will probably desire extremely large *positive* values of the composite bulk modulus. To attain these, B_1 must be slightly *more* negative than Eq. (2.9), but the linearized solution derived here shows that B_1 cannot pass through the value given in Eq. (2.9) without all the elastic fields becoming infinite. In the next section, we show via a full finite deformation re-analysis of the same problem that even a small amount of constitutive nonlinearity will remove this pathology and permit B_1 to decrease below the value in Eq. (2.9), while the full solution remains well behaved; this, legitimizes in principle the formation of composite materials with extremely large *positive* bulk modulus.

2.3.2. Solutions within finite elasticity theory

As the results of the previous section show, the presence of an inclusion with a sufficiently negative bulk modulus to produce a large effective modulus for the composite has the effect of producing strains in the inclusion and in the matrix near the inclusion that are very large compared to the average strains in the composite. The linearized elasticity solution also has the feature noted in the previous section that all elastic fields become infinite everywhere in the composite sphere for a certain negative value of the inclusion bulk modulus. It seems worthwhile to examine whether, and if so how, these behaviors are modified by a full finite deformation solution. Thus, in this section we provide analytical finite deformation solutions of the same problems treated in the previous section. The ability to obtain closed-form analytical solutions within a finite deformation formulation is due to our choice of a special type of constitutive model, namely the generalization to three dimensions (Ogden, 1984) of the "harmonic material" constitutive equation originally devised by John (1960). The analysis to follow builds on that presented by Ogden (1984), who solved the spherically symmetric deformation of a spherical shell.

The constitutive equation we employ is expressed in terms of the Biot stress tensor $\mathbf{T}$, which is the reference-configuration stress measure that is work-conjugate to the right stretch tensor $\mathbf{U}$ in the polar decomposition of the deformation gradient tensor, $\mathbf{F} = \mathbf{R} \cdot \mathbf{U}$, where $\mathbf{R}$ is the rotation tensor. The strain measure that is work-conjugate to the Biot stress is the right-stretch strain tensor, $\mathbf{E} \equiv \mathbf{U} - \mathbf{I}$, where $\mathbf{I}$ is the second-rank identity tensor. The Biot stress $\mathbf{T}$ is related to the nominal stress tensor $\mathbf{S}$ as

$$\mathbf{T} = \tfrac{1}{2}(\mathbf{S} \cdot \mathbf{R} + \mathbf{R}^{\mathrm{T}} \cdot \mathbf{S}^{\mathrm{T}}). \tag{2.16}$$

The elastic constitutive equation thus takes the form

$$\mathbf{T} = \frac{\partial W}{\partial \mathbf{U}}, \tag{2.17}$$

with the strain energy function $W(\mathbf{U})$ that is the three-dimensional generalization of John's harmonic materials (Ogden, 1984)

$$W = F(I_1) - c_1 I_2 + c_2 I_3, \tag{2.18}$$

where I_1, I_2, I_3 are the principal invariants of $\mathbf{U}$, $F(I_1)$ is a function to be specified shortly, and c_1, c_2 are constants. For the spherically symmetric problems to be analyzed, the reference configuration spherical coordinates are R, Θ, Φ, while the current configuration spherical coordinates are r, θ, ϕ. We show in Appendix A that the general spherically symmetric solution of the equilibrium finite deformation governing equations for this material is

$$u_R = \alpha R + \frac{\beta}{R^2} \tag{2.19}$$

$$E_{RR} = \alpha - 2\frac{\beta}{R^3}, \quad E_{\Theta\Theta} = E_{\Phi\Phi} = \alpha + \frac{\beta}{R^3}. \tag{2.20}$$

We emphasize that the above are the general solutions for arbitrary $F(I_1)$.

Within the finite deformation formulation, we shall wish to examine both the case of a linear stress–strain constitutive relation and a nonlinear one, since solutions from each of these will aid understanding. Thus, for simplicity we choose the strain energy function (2.18) to be at most cubic in the principal stretches, with $F(I_1)$ having the specific form:

$$F(I_1) = d_1 I_1^3 + d_2 I_1^2 + d_3 I_1 + d_4 \;\Rightarrow\; F'(I_1) = 3d_1 I_1^2 + 2d_2 I_1 + d_3, \tag{2.21}$$

where $d_1 - d_4$ are constants. In addition, we apply the requirements of a stress-free reference configuration, and we choose the constants in our finite deformation constitutive equation so that the stress–strain equations reduce to the small-displacement-gradient constitutive equations when strains are infinitesimal. After a final renaming of constants, we show in Appendix A that the resulting stress–strain expressions are [which give the stress field solution upon substitution of Eq. (2.20)]:

$$T_{RR} = \left(B + \frac{4}{3}G\right) E_{RR} + 2\left(B - \frac{2}{3}G\right) E_{\Theta\Theta} + P(E_{RR} + 2E_{\Theta\Theta})^2 + QE_{\Theta\Theta}^2,$$

$$T_{\Theta\Theta} = T_{\Phi\Phi} = \left(B - \frac{2}{3}G\right) E_{RR} + 2\left(B + \frac{1}{3}G\right) E_{\Theta\Theta} + P(E_{RR} + 2E_{\Theta\Theta})^2 + QE_{RR}E_{\Theta\Theta}. \tag{2.22}$$

Let us first consider the case of a linear constitutive equation within the finite deformation formulation; this means that we choose $P = Q = 0$ [which means choosing $c_2 = d_1 = 0$ in the constitutive model Eq. (2.18) with Eq. (2.21)]. One then observes from Eqs. (2.19), (2.20) and (2.22) that the solution form for the stress, strain and displacement fields is identical to those derived within the infinitesimal-displacement-gradient formulation, Eqs. (2.2)–(2.4). Thus, the solutions to the two composite sphere

problems will also be identical. Therefore, accounting for finite deformations but still retaining a linear constitutive relationship, at least for the constitutive class treated, does not alter the phenomena and conclusions drawn from the infinitesimal elasticity solution.

Now let us consider finite deformation solutions to the composite sphere problem when the constitutive equation is also nonlinear, having the special form described in this section which leads to the stress–strain relations Eq. (2.22). The effects that we wish to illustrate will still be apparent if we continue to assume that the *inclusion* material has a linear constitutive equation, so that the only constitutive nonlinearity is present in the matrix material. This means that P and Q are only nonzero in the matrix material. Here, we will solve the finite deformation counterpart of Problem 2 considered previously, namely that of prescribed uniform radial displacement on the outer sphere boundary of the composite. The four conditions we apply are the same as those applied earlier, namely zero displacement at the center of the spherical inclusion, continuity of displacement and traction across the inclusion/matrix interface, and a uniform prescribed radial displacement of magnitude u on the outer boundary. Imposing the above four conditions on the solution fields Eqs. (2.19), (2.20) and (2.22) enables one to solve for the four undetermined constants appearing in these fields; the results are:

$$\alpha_1 = \frac{-(b^3-a^3)[3a^3(B_1-B_2)-b^3(3B_1+4G_2)]+18a^3b^2Pu \pm (b^3-a^3)s}{D},$$

$$\beta_1 = 0, \quad \alpha_2 = \frac{3a^6(B_1-B_2)-a^3b^2(3bB_1+4bG_2+2Qu)+2b^5Qu \mp a^3 s}{D},$$

$$\beta_2 = a^3b^2\frac{b^3(3bB_1+4bG_2-2Qu)+a^3(-3bB_1+3bB_2+18Pu+2Qu) \pm bs}{D}, \tag{2.23}$$

where

$$D = 18a^6P + 2(a^3-b^3)^2Q,$$

$$s = \sqrt{\begin{array}{l}[b^3(3B_1+4G_2)-3a^3(B_1-B_2)]^2+36a^3b^2(3B_1+4G_2)Pu \\ \quad -4b^2(b^3-a^3)(3B_2+4G_2)Qu-36b^4PQu^2.\end{array}}$$

Notice that these solutions have a denominator, D, that is independent of the elastic coefficients of the linear terms in the stress–strain equations. Therefore, these results show that, unlike the solutions for the linear constitutive equation, the solution fields will remain finite everywhere in the composite even when B_1 passes through the critical negative value that causes the effective bulk modulus to switch from very large negative values to very large positive ones. This implies that in an actual elastic material, in which one might expect some nonlinearity in the stress–strain equations, one should be able to lower B_1 below the critical negative value predicted by the linearized analysis

without pathological behavior of the composite. The resulting composite will then have extremely large *positive* bulk modulus for infinitesimal deformations.

Let us illustrate the results of the above solution for a specific choice of the composite parameters. We choose parameter values to be the same as those of the linearized solution illustrated in Fig. 4, namely $V_1 = 0.01$, $v_2 = 0.2$, but we now choose the inclusion bulk modulus to equal the value that causes the linearized solution to become singular, namely $B_1 = -1.0202B_2$. In addition, we choose rather small values for the nonlinear coefficients, namely $P = B_2/30$ and $Q = -3B_2/20$, and consider an imposed displacement $u = b/1000$. In this case, the solution set Eq. (2.23) reduces to

$$\{\alpha_1, \beta_1, \alpha_2, \beta_2\} = \{-0.1998, 0, 0.003016, -0.002016b^3\},$$
$$\{0.2022, 0, -0.001020, 0.002020b^3\}. \tag{2.24}$$

Note that with these values of the constants, the solutions for the displacement, strain and stress fields, given by Eqs. (2.19), (2.20) and (2.22) are all well behaved and have finite values everywhere in the composite, in contrast to the linearized elasticity solution which would predict that the fields are infinite everywhere in the composite. The displacement and strain fields for the present solution have the same forms as those shown in Fig. 4. Since the present problem is constitutively nonlinear, the composite bulk modulus will change with the applied load or applied displacement level. For the example parameter values used above, the composite secant bulk modulus for the solution resembling the linear elastic solution is $\bar{B} = 5.08B_2$. The finite deformation solution of Problem 1 considered previously also has fields that are well behaved everywhere and also permits large bulk modulus values; it is omitted here for space reasons. Although not within the scope of the present work, we remark that incorporation of a small amount of linearly viscoelastic dissipation also has the effect of eliminating the singularities while retaining the possibility of extreme material properties (Lakes, 2001b).

2.4. Distributed three-dimensional composites

We now consider the effect of phases of negative stiffness in several three-dimensional composites for which elasticity solutions are known. First, in this section we discuss composite materials obeying the following Hashin–Shtrikman (1963) formulae, which are attainable via known microstructures for which there are exact analytical solutions within the theory of elasticity:

$$G_c = G_2 + \frac{V_1}{1/(G_1 - G_2) + 6(B_2 + 2G_2)V_2/[5(3B_2 + 4G_2)G_2]}, \tag{2.25}$$

$$B_c = B_2 + \frac{V_1(B_1 - B_2)(3B_2 + 4G_2)}{(3B_2 + 4G_2) + 3(B_1 - B_2)V_2}. \tag{2.26}$$

Here, B_1, G_1, V_1 and B_2, G_2, V_2 are the bulk modulus, shear modulus and volume fraction of phases 1 and 2, respectively. The bulk modulus formula Eq. (2.26) was shown by Hashin (1962) to be the exact solution for a hierarchical microstructure

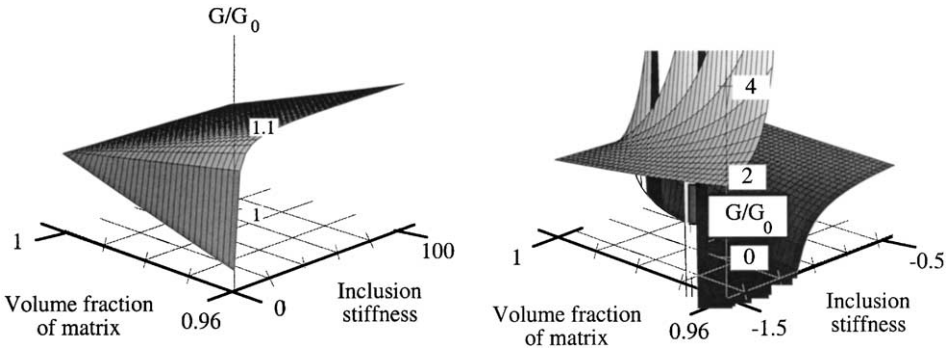

Fig. 5. Stiffness of Hashin–Shtrikman composite. Inclusion and composite shear modulus normalized to matrix shear modulus G_0. Left, positive inclusion stiffness; right, negative inclusion stiffness.

of coated spheres of different sizes in which the outer layer (phase 2) radius and core (phase 1) radius have a specified ratio for all inclusions. The construction is based on a solution for spherical symmetry due to Love (1944). The coated sphere is a neutral inclusion in that it does not disturb the assumed hydrostatic stress state in the surrounding medium, assumed to have a bulk modulus equal to that of the coated inclusion. The composite is made by adding inclusions of progressively smaller size until the space is filled. As elucidated by Milton and Serkov (2001) and Milton (2001), since the stress and strain fields are undisturbed in the process, the loads and displacements at the boundary are undisturbed; hence, the effective bulk modulus of the medium remains unchanged by the progressive addition of inclusions. Exact attainment of Eq. (2.25) is possible via a hierarchical laminate morphology (Francfort and Murat, 1986; Milton, 1986). We remark that these formulae are familiar to many in the context of bounds: they are bounds if both constituents have positive stiffness. For present purposes, we are not concerned with bounds, but with the fact that Eqs. (2.25) and (2.26) are exact elasticity solutions for known microstructures and the fact that these exact solutions remain valid for negative stiffness constituents.

Calculated stiffness of a Hashin–Shtrikman composite governed by Eq. (2.25) as a function of volume fraction and the stiffness of one constituent is shown in Fig. 5. If the inclusions are stiff, a small concentration of them does not stiffen the composite very much, as is well known. If, however, the inclusions have the correct value of negative stiffness, the composite stiffness becomes arbitrarily large, tending to infinity. For example, the composite shear modulus given by Eq. (2.25) becomes infinite for inclusions of (negative) shear modulus $G_i \approx -1.1G_m$ for a matrix Poisson's ratio of 0.3 and an inclusion volume fraction of 0.01. Rationale for the possibility of particles of negative shear modulus is presented in Section 4.3 and experimental justification is adduced in Section 5. Observe the difference in scale of the vertical axes in Fig. 5a and b. Such a composite is not governed by the bounding theorems, since nonnegative internal energy is not assumed here, in contrast to the bounding calculation. The present analysis does not depend on any assumptions related to bounds. Rather, it makes use of attainable closed-form expressions for composite properties. The plots have similar

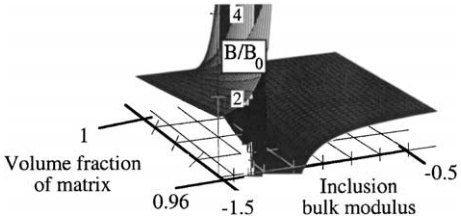

Fig. 6. Stiffness of Hashin–Shtrikman composite. Inclusion and composite bulk modulus normalized to matrix bulk modulus B_0.

shape to those for resonance phenomena. They are not resonances since there are no inertial terms. As with a resonance, there are terms of opposite sign in the denominator, but in the present case they have a quasistatic origin. The negative stiffness approach is distinct from the use of structural resonance to achieve high dielectric properties (Nicorovici et al., 1994), since there are no inertial terms in the continuum elasticity equations used in the present work.

The composite bulk modulus given by Eq. (2.26) becomes singular for inclusions of negative bulk modulus $B_i \approx -1.35B_m$. The behavior is shown in Fig. 6. The location of the singularity depends on the Poisson's ratio of the matrix.

2.5. Variational principle estimates for the effective modulus tensor of three-dimensional random composites having a negative stiffness phase

In this section, we show that an existing variational principle that provides estimates for the overall elastic modulus for random composite materials remains valid when one of the composite's phases has negative stiffnesses, and we further show that the estimates from this variational principle also exhibit the feature that the composite stiffnesses can be made extremely large by suitable choice of the moduli of the negative stiffness phase.

For simplicity, let us consider here an infinite linear elastic composite body consisting of firmly bonded phases that is loaded only by a body force distribution $\boldsymbol{f}(\mathbf{x})$. Following Hashin and Shtrikman (1962a, b), Willis (1977) showed that the governing equations of linear elasticity for the stress and infinitesimal strain tensor fields $\boldsymbol{\sigma}, \boldsymbol{\varepsilon}$, and the displacement vector field $\mathbf{u}$, can be recast in the following way: One introduces a *homogeneous* "comparison" body with moduli (independent of position $\mathbf{x}$) $\mathbf{L}_0$ [and having solutions $\boldsymbol{\sigma}_0(\mathbf{x}), \boldsymbol{\varepsilon}_0(\mathbf{x})$, to the same applied $\boldsymbol{f}(\mathbf{x})$], so that

$$\boldsymbol{\sigma}(\mathbf{x}) = \mathbf{L}_0\boldsymbol{\varepsilon}(\mathbf{x}) + \boldsymbol{\tau}(\mathbf{x}), \quad \boldsymbol{\tau}(\mathbf{x}) \equiv [\mathbf{L}(\mathbf{x}) - \mathbf{L}_0]\boldsymbol{\varepsilon}(\mathbf{x}), \tag{2.27}$$

where the second equation defines the "stress polarization" tensor field $\boldsymbol{\tau}(\mathbf{x})$. The solution to the elasticity field equations can then be shown to involve solution of the following integral equation for $\boldsymbol{\tau}(\mathbf{x})$:

$$(\mathbf{L}(\mathbf{x}) - \mathbf{L}_0)^{-1}\boldsymbol{\tau}(\mathbf{x}) + \int \boldsymbol{\Gamma}_0(\mathbf{x} - \mathbf{x}')\boldsymbol{\tau}(\mathbf{x}')\,\mathrm{d}\mathbf{x}' = \boldsymbol{\varepsilon}_0(\mathbf{x}), \tag{2.28}$$

where $\mathbf{\Gamma}_0(\mathbf{x})$ is a fourth-rank tensor field that is two spatial derivatives of the infinite-homogeneous-body (i.e., comparison body) Green's function.

The important fact for our present purposes is that Willis (1977) proved that self-adjointness of Eq. (2.28) arises solely from the usual index symmetries of the actual elastic modulus tensor $\mathbf{L}(\mathbf{x})$ and the comparison modulus tensor $\mathbf{L}_0$, and that this self-adjointness immediately implies from Eq. (2.28) the Hashin–Shtrikman (stationary) variational principle

$$\delta\left\{\int\left[\boldsymbol{\tau}(\mathbf{x})(\mathbf{L}(\mathbf{x})-\mathbf{L}_0)^{-1}\boldsymbol{\tau}(\mathbf{x})\right.\right.$$

$$\left.\left.+\boldsymbol{\tau}(\mathbf{x})\int\mathbf{\Gamma}_0(\mathbf{x}-\mathbf{x}')\boldsymbol{\tau}(\mathbf{x}')\,\mathrm{d}\mathbf{x}'-2\boldsymbol{\tau}(\mathbf{x})\boldsymbol{\varepsilon}_0(\mathbf{x})\right]\,\mathrm{d}\mathbf{x}\right\}=0. \tag{2.29}$$

Therefore, this variational principle is valid even when one of the phases of the composite has negative stiffnesses, so long as the actual and comparison elastic modulus tensors have the usual index symmetries, and provided that the comparison modulus tensor is chosen such that a Green's function exists for the body.

Willis (1982) has shown how to apply Eq. (2.29) to random composite materials. Retaining up through two-point statistical information, and assuming statistical uniformity and ergodicity of the composite, he deduced the stochastic form of Eq. (2.29). Making, for simplicity, the further assumption of isotropic *distribution* of the phases, Willis (1982) showed that the stochastic form of Eq. (2.29) gives the following estimate for the effective modulus tensor of the random composite material having n phases each with modulus tensor $\mathbf{L}_r$:

$$\tilde{\mathbf{L}}=\left\{\sum_{r=1}^{n}V_r[\mathbf{I}+(\mathbf{L}_r-\mathbf{L}_0)\mathbf{P}]^{-1}\right\}^{-1}\sum_{s=1}^{n}V_s[\mathbf{I}+(\mathbf{L}_s-\mathbf{L}_0)\mathbf{P}]^{-1}\mathbf{L}_s. \tag{2.30}$$

Here, $\mathbf{I}$ is the fourth-rank identity tensor and the constant fourth-rank tensor $\mathbf{P}$ is given in terms of the Fourier transform of $\mathbf{\Gamma}_0(\mathbf{x})$ as

$$\mathbf{P}\equiv\frac{1}{4\pi}\int_{|\boldsymbol{\xi}|=1}\tilde{\mathbf{\Gamma}}_0(\boldsymbol{\xi})\,\mathrm{d}S. \tag{2.31}$$

Result (2.30) is thus a variational estimate valid for composites having a negative stiffness phase. To be completely explicit, we now consider two-phase composites consisting of an isotropic matrix containing a random distribution of isotropic inclusions (of arbitrary shape). In this case, Eq. (2.30) simplifies to give the following variational estimates for the overall bulk and shear modulus of the composite:

$$\tilde{B}=\frac{4G(V_1B_1+V_2B_2)+3B_1B_2}{4G+3(V_1B_2+V_2B_1)},$$

$$\tilde{G}=\frac{G(9B+8G)(V_1G_1+V_2G_2)+6(B+2G)G_1G_2}{G(9B+8G)+6(B+2G)(V_1G_2+V_2G_1)}, \tag{2.32}$$

where subscripts 1, 2 indicate inclusion and matrix, respectively, and the unsubscripted quantities are the comparison moduli. [Incidentally, for composites whose phases are

all positive definite, the standard Hashin–Shtrikman lower (upper) bounds follow from Eq. (2.32) by choosing the comparison moduli to equal the smallest (largest) of the constituent moduli.]

Let us consider specifically a composite consisting of a positive definite matrix phase containing inclusions of negative stiffness. One permissible and sensible choice for the comparison moduli is that they equal the matrix moduli. Then Eqs. (2.32) show that the variational estimates of the bulk and shear moduli can be made to be arbitrarily large by suitable (negative) choice of the inclusion moduli; the variational estimates of the bulk and shear moduli become infinite when the inclusion moduli take on the (negative) values:

$$B_1 = -\frac{4G_2 + 3V_1B_2}{3V_2}, \quad G_1 = -G_2\frac{3(3+2V_1)B_2 + 4(2+3V_1)G_2}{6V_2(B_2+2G_2)}. \tag{2.33}$$

Note from these results that if a composite having only an extremely high bulk modulus were sought, this could be accomplished with inclusions of strongly elliptic material: the inclusion bulk modulus would need to have a value close to that given by the first equation of Eq. (2.33), but its shear modulus could be chosen positive and sufficiently large that the strong ellipticity requirement ($B_1 > -4G_1/3$) were met (see the discussion in Section 4.3).

2.6. Discussion

It is interesting to note that all three of the formulae we have derived and presented for the effective bulk modulus in the present Section 2, namely, Eqs. (2.8), (2.26) and (2.32) [if the comparison moduli are chosen equal to the matrix moduli in Eq. (2.32), as we have suggested is sensible] are *identical*. This is also true of the two formulae presented for the effective shear modulus, namely, Eqs. (2.25) and (2.32) [again with comparison moduli equal to matrix moduli in the latter]. Thus, these formulae describe the effective modulus behavior in a variety of different situations: for example, we have shown that the effective bulk modulus arises from the exact elasticity solutions of a single composite sphere and of Hashin's (1962) composite material comprised of a hierarchical microstructure of coated spheres, as well as from a variational estimate for a random two-phase composite material having arbitrary inclusion shape under the assumptions explained in Section 2.5. Our conclusions on the production of a high composite stiffness by having a phase of appropriate negative stiffness are therefore applicable to this full range of situations, with in fact *quantitatively identical* choices of the negative moduli because of the just-mentioned concurrence of the formulae.

3. Negative stiffness constituents

3.1. Physical concept. Distinction between negative stiffness and negative Poisson's ratio

Negative stiffness entails a reversal of the usual directional relationship between force and displacement in deformed objects. Ordinarily (positive stiffness), the force

applied to a deformable object (such as a spring) is in the same direction as the deformation, corresponding to a restoring force which tends to restore the spring to its neutral position. Negative stiffness involves unstable equilibrium, hence a positive stored energy at equilibrium.

Negative stiffness is to be distinguished from negative Poisson's ratio. In the 17th century, S.D. Poisson observed that a material stretched under axial tensile forces not only elongates longitudinally, but it also contracts *laterally*. Poisson's ratio, represented by v, is defined as the negative lateral strain of a stretched or compressed body divided by its longitudinal strain. Poisson's ratio is dimensionless, and for most solids its value ranges between 0.25 and 0.33 (Timoshenko, 1983). For most foams (Gibson and Ashby, 1988), Poisson's ratio is about 0.3. However, rubbery materials can have values close to 0.5, which is the upper limit for stability of isotropic materials. Lakes (1987) and co-workers have conceptualized, fabricated and studied negative Poisson's ratio foams with v as small as -0.8. These materials become fatter in cross section when they are stretched. Other workers have found single crystals, laminates, and other materials which have a negative Poisson's ratio, as reviewed by Lakes (1993). For isotropic materials, a Poisson's ratio in the range -1 to 0.5 is associated with stability, while a negative stiffness material is unstable in bulk form.

3.2. Lumped examples of negative stiffness

Examples of negative stiffness are known in the context of certain structures and objects (Bazant and Cedolin, 1991). For example, consider a column which has been constrained in a buckled "S" shaped configuration (Fig. 7a). By pressing laterally on the column, one can cause it to snap through. The negative stiffness condition is unstable, but the column can be stabilized by a lateral constraint, such as by connecting it to a rigid block. One can easily verify the properties of the buckled column with the aid of a flexible plastic ruler.

Negative stiffness occurs in single-cell models of foam materials. In particular, flexible tetrakaidecahedral models exhibit a force–deformation relation which is not monotonic in compression (Rosakis et al., 1993). The cells bulge inwardly during high compressive strain, giving rise to a geometric nonlinearity.

Negative stiffness also occurs in the lumped cell shown in Fig. 7b. This consists of stiff rotatable nodes with pre-strained springs. If the pre-strain is sufficient, the effective shear modulus of the cell is negative. Such a two-dimensional lattice structure, originally examined in a study of generalized continuum mechanics but not for unusual values of the classical moduli (Berglund, 1977), can give rise to negative Poisson's ratio (Lakes, 1991) and even negative shear moduli, provided sufficient pre-strain is incorporated. The structure is two-dimensionally cubic; however, it is possible to obtain elastic isotropy by suitable choice of the stiffnesses of the elastic ligaments. Given the elastic constants provided in Berglund (1977), we invoke isotropy, and calculate the engineering elastic constants in terms of the node size and the relative magnitude of the noncentral forces. In the following description of the lattice, node radius is r, lattice spacing is d, $k_1 =$ spring constant, $k_2 =$ diagonal spring constant, $k_3 =$ band spring constant for noncentral force. The h's are natural spring lengths and f is a pre-compression factor.

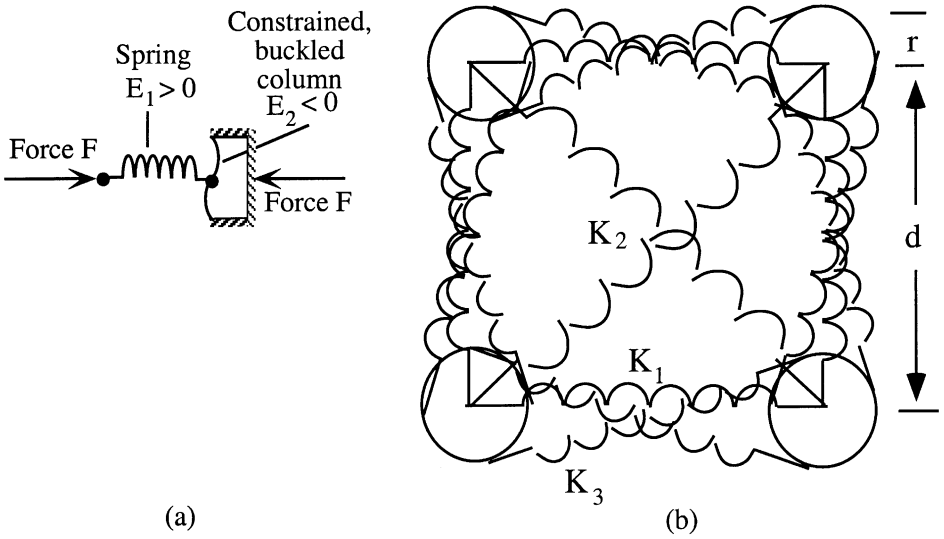

Fig. 7. (a) A lumped Reuss model. A negative stiffness element of effective modulus E_2, represented by a constrained, buckled column is in series with a spring, which is an element of positive stiffness. (b) A lumped cell consisting of stiff rotatable nodes with pre-strained springs. If the pre-strain is sufficient, the shear modulus of the cell is negative.

The resting length of the oblique bands is

$$L_0 = \sqrt{d^2 - 4r^2}.$$

The initial length of spring element 2 is related to the pre-strain f by

$$h_2 = d(1 - \mathrm{f})\sqrt{2}.$$

The condition for isotropy is

$$k_3 = \frac{k_2(1 + \frac{1}{2}(1/h_2)\{h_2 - d\sqrt{2}\}) - (d/\sqrt{2}h_2)k_1}{2(L_0 - h_3)L_0/d\sqrt{2}h_2 + \sqrt{2}h_3(L_0^2 - 4r^2)/L_0h_2d}.$$

The shear modulus is

$$G = k_1 + k_2\left(2 - \frac{3h_2}{d\sqrt{2}}\right) + k_3\left(2 - 8\frac{r^2}{d^2}\frac{h_3}{L_0}\right).$$

Since one may freely vary the pre-strain, a sufficiently large choice of the natural length h_3 (for nonzero node size r) clearly gives a negative shear modulus G.

3.3. Distributed examples of negative stiffness

Materials in the vicinity of certain phase transformations are expected to exhibit negative stiffness on a micro-scale for the following reasons. Ferroelastic (Salje, 1990) and ferroelectric materials (Lines and Glass, 1979; Cady, 1964) in the vicinity of phase transformations exhibit stiffness components which achieve a minimum or tend to zero

at a critical temperature. Below the critical temperature a domain or band structure appears. Domains may be from several millimeters to tens of micrometer in size. These phase transformations have been analyzed via a modified (Falk, 1980, 1983) Landau theory in which the free energy $\mathbf{F}$ depends on strain $\boldsymbol{\varepsilon}$ and temperature T as follows:

$$\mathbf{F} = \alpha\boldsymbol{\varepsilon}^6 - \beta\boldsymbol{\varepsilon}^4 + \gamma(T - T_1)\boldsymbol{\varepsilon}^2, \tag{3.1}$$

with α, β, γ and T_1 as positive constants depending on the material. Define a normalized temperature,

$$T_n = \frac{\alpha\gamma}{\beta^2}(T - T_1) - \frac{1}{4}. \tag{3.2}$$

The free energy is seen to have a single relative minimum at high temperature $T_n > 1/12$, three relative minima at intermediate temperature $-1/4 < T_n < 1/12$, and two relative minima separated by a maximum at low temperature $T_n < -1/4$. This maximum at a strain of zero represents unstable equilibrium. Formally, the stress–strain relation is $\sigma = \partial F/\partial\varepsilon$. At low temperature, the effective stiffness is negative. One does not ordinarily speak of it in that way in the context of ferroelastic or shape memory materials since that condition is unstable. As the temperature is lowered, a spontaneous strain appears, corresponding to a shift from the "center" position of unstable equilibrium to one of the stable points of minimum energy. The material acquires a structure of domains or bands. The poly-domain material has a positive stiffness. Formation of bands has been understood via continuum elasticity (Knowles and Sternberg, 1978) in which stress–strain behavior has a non-monotonic portion. The domain walls require energy to form; therefore, particles of sufficiently small size (from micrometer to centimeter scale depending on the material) are observed to be single domain (Salje, 1990). Such single domains are expected to exhibit negative stiffness. Experimental results regarding inference of negative stiffness are reported elsewhere (Lakes, 2001a; Lakes et al., 2001).

Foam materials under heavy compression have a macroscopic positive stiffness; however, they develop a band structure when heavily compressed, and this band structure is related to stability of the individual cells (Rosakis et al., 1993). The transformation to a banded structure is linked to buckling of the foam cell ribs, which also gives rise to a nonlinear stress–strain characteristic. From the band structure, one may infer negative stiffness on the local scale via the analysis discussed below. Negative stiffness has been observed experimentally in single-cell models as discussed above.

4. Stability considerations

4.1. Overview

Since a negative stiffness constituent alone is unstable, we provide here a preliminary discussion of the stability of a composite having a negative stiffness constituent. This instability of a negative stiffness material may be understood as follows. Consider a block of material. Perturb the block slightly with a small force. If the block has positive

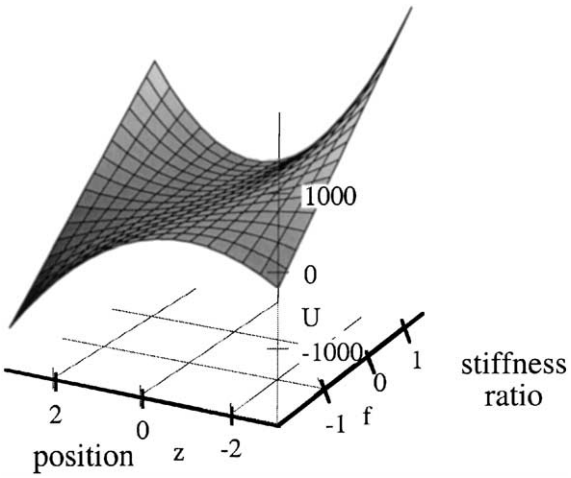

Fig. 8. Reuss composite. Internal energy U (arbitrary units) vs. position coordinate z (arbitrary units) and dimensionless stiffness parameter f, the ratio of stiffness of the two phases.

stiffness, it will resist the deformation with an opposing force. If the stiffness is negative, the block exerts a force in the same direction as the perturbation, creating a divergent, unstable condition.

4.2. Stability of lumped one-dimensional model

If no external constraint is applied, the Reuss model (Fig. 7a) with a negative stiffness phase (such as the post-buckled column in Fig. 7a) is unstable because the spring end (at left in Fig. 7a) is free. Since the spring supplies no force, the model is equivalent to the negative stiffness portion alone.

Consider a constrained Reuss model in which the force in Fig. 7a is supplied by a hard constraint. To evaluate the stability of this model, consider the internal energy U as it depends on coordinates related to deformation. In the following, E_1 is a positive stiffness (a spring), z is the position of the joint between the spring and buckled column, and f is a dimensionless scaling parameter which can assume positive or negative values, with negative values corresponding to the buckled column element; the 1/2 refers to a 50% "volume fraction" in the lumped system:

$$U = \tfrac{1}{2}E_1(1-z)^2 + \tfrac{1}{2}fE_1z^2. \tag{4.1}$$

As shown in Fig. 8, the internal energy U is concave up as a function of z, provided that $f > -1$. Therefore, some Reuss composites with a negative stiffness constituent are stable when constrained. Behavior of a Reuss model (Fig. 8) has a singularity as shown in Fig. 9. The Reuss model with a single element of each phase is to be distinguished from the Reuss composite which has multiple elements. Some theoretical studies have been conducted of chains of elements with nonmonotone stress–strain relations (Balk et al., 2001); slow deformation leads to a vibrating steady state with radiation of

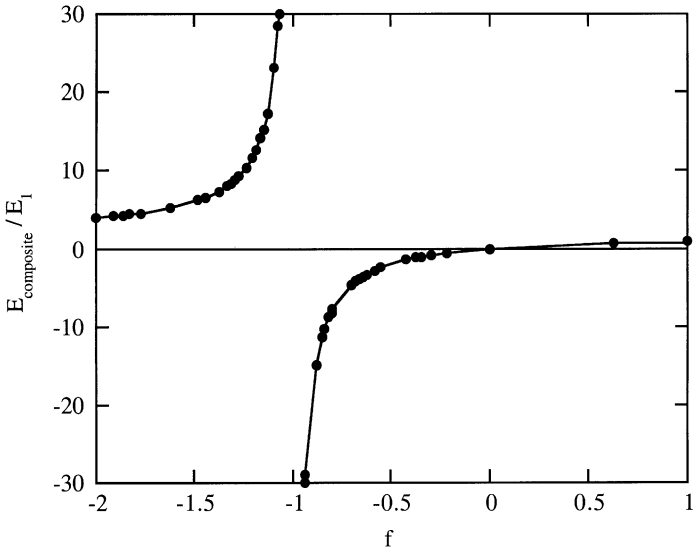

Fig. 9. Reuss composite, 50% volume fraction. Composite stiffness normalized to stiff phase stiffness vs. dimensionless stiffness parameter f.

energy in the elastic case, or hysteresis in the viscoelastic case. Such elements have also been called bi-stable elements (Puglisi and Truskinovsky, 2000). Such chains are not equivalent to a Reuss composite since each element is bi-stable, or equivalently, has negative stiffness. A Reuss composite with multiple elements will likely exhibit different stability conditions from a single-cell model, at least under the assumption that each lamina has moduli exactly equal in magnitude. Non-monotonic force–deformation relations have also been explored in continuous media from the perspective of applied mathematics (James, 1979; Ball, 1996). Negative stiffness of large magnitude is possible in a constrained Reuss model. For many applications, that may not be as useful as a positive composite stiffness. However, the regime for which Reuss composite stiffness tends to positive infinity is unstable. So Reuss composites cannot be used to achieve a large *positive* stiffness greater than that of the constituents. Three-dimensional aspects of Reuss-type laminates were considered by Gutierrez (1999), who explored regimes of stability for such microstructures.

4.3. Stability of materials viewed as continua

There are several ranges of elastic constants which are associated with stability of elastic materials on various levels. We consider first the case of infinitesimal homogeneous isotropic linear elastic deformations from an unstrained state. The strain energy is positive definite if and only if the shear modulus G and Poisson's ratio v satisfy (e.g., Timoshenko and Goodier, 1970)

$$G > 0 \quad \text{and} \quad -1 < v < 0.5. \tag{4.2}$$

Materials that obey these relations give rise to unique solutions of mixed boundary-value problems in which any appropriate combination of surface tractions and surface displacements is specified. Hill (1957) showed that uniqueness is a necessary condition for incremental stability; such materials do produce stable solutions for large classes of mixed boundary-value problems. Based on these facts, we recognized that it would be possible to prepare materials with a negative Poisson's ratio which would be stable with no external constraint. In view of that fact, negative Poisson's ratio materials were prepared in our laboratory (Lakes, 1987). Inequality Eq. (4.2) implies that E, G, and B must be positive for positive definiteness of the strain energy and for an *unconstrained* block of material to be *globally* stable under small deformation for a wide range of loading conditions.

Boundary-value problems for which *purely displacement* boundary conditions are prescribed have unique solutions (Cosserat, 1898) that are also incrementally stable (Lord Kelvin, 1888) if the elastic moduli are strongly elliptic:

$$G > 0 \quad \text{and} \quad -\infty < \nu < 0.5 \quad \text{or} \quad 1 < \nu < \infty. \tag{4.3}$$

This range is considerably less restrictive than the range in inequality Eq. (4.2). Physically, the displacement boundary condition corresponds to a *constraint* on the elastic object. That constraint makes for stability, hence a less restrictive range of admissible elastic constants. [Truesdell and Noll (1965) have further shown that a homogeneous, arbitrarily anisotropic body in a homogeneously (finitely) strained configuration subject to purely displacement boundary conditions has a unique and stable solution for superimposed infinitesimal deformation if the strained state elastic modulus tensor is strongly elliptic.]

In terms of the Lamé moduli λ and G, the strong ellipticity conditions (4.3) are

$$G > 0 \quad \text{and} \quad \lambda + 2G > 0. \tag{4.4}$$

The physical significance of the $\lambda + 2G > 0$ condition is that the stiffness, which can also be considered as the tensorial modulus C_{1111}, is positive for axial compression or extension under lateral constraint (uniaxial *strain*). When Eq. (4.4) is satisfied, the speed of longitudinal waves is positive. Inequality Eq. (4.4) is equivalent to (Timoshenko, 1983)

$$G > 0, \quad \frac{E(1-\nu)}{(1+\nu)(1-2\nu)} = 2G\frac{(1-\nu)}{(1-2\nu)} > 0. \tag{4.5}$$

Since $E = 2G(1+\nu)$, the range of E for strong ellipticity is $-\infty < E < \infty$. As for the bulk modulus,

$$B = \frac{2G(1+\nu)}{3(1-2\nu)} \tag{4.6}$$

or equivalently $B = \lambda + 2G/3$, so that for strong ellipticity $-4G/3 < B < \infty$. So the condition of strong ellipticity allows some moduli to be negative. If strong ellipticity is violated, the material may exhibit an instability associated with the formation of bands of heterogeneous deformation (Knowles and Sternberg, 1978). Note that the specific examples of achieving extremely high composite *bulk* modulus exhibited in Section 2

required a negative bulk inclusion modulus that need not violate strong ellipticity in the inclusion.

Our earlier examples of achieving extremely high composite *shear* modulus require a negative shear modulus in the inclusions, which does violate the strong ellipticity condition *in the inclusions*. However, the violation of strong ellipticity does not guarantee the loss of stability of the inclusions: experiments show that, for example in ferroelastic (Salje, 1990) and ferroelectric (Lines and Glass, 1979; Cady, 1964) materials, the energy penalty of band formation suppresses banding when particles of the material are sufficiently small. Thus in these examples and others, an instability criterion based purely on elasticity theory may not contain enough of the physics of the actual material behavior, and hence may predict instabilities in regimes where such do not occur in reality. Negative shear modulus can also occur in lumped elements which cannot form bands and for which continuum conditions of ellipticity do not apply. A full accounting of shear properties with single domains would necessarily incorporate both anisotropy of the crystal and surface energy. Furthermore, the experiments of Lakes et al. (2001) involve inclusions having a negative shear modulus, yet the measured dramatic increase in complex composite shear modulus shows that they must *not* be experiencing a banding instability.

In summary, negative stiffness is not excluded by any physical law. Objects with negative stiffness are unstable if they have free surfaces. They can be stabilized if they are constrained rigidly or by an elastic composite matrix. A continuum with a negative bulk modulus is stable if constrained. Negative shear modulus in a continuum can give rise to a banding (domain) instability associated with loss of ellipticity, but such an instability does not always occur when strong ellipticity is violated.

4.4. Stability of three-dimensional composite

We consider the elastic moduli and Poisson's ratio of composites which attain the lower Hashin–Shtrikman formulae. As shown in Fig. 10, significant enhancements in stiffness are obtained within the stability limits -1 to 0.5 on the *composite* Poisson's ratio, corresponding to the shear and bulk moduli of the composite being positive. The critical inclusion modulus values for stability and for singularities depends on the assumed concentration and Poisson's ratio of the inclusions and the Poisson's ratio of the matrix.

5. Discussion

Possible uses of composites with inclusions of negative stiffness are as follows. They may be used in studying properties of single domains of ferroelastic, ferroelectric, shape memory martensite or ferromagnetic materials. A dilute concentration is sufficient to obtain substantial effects; therefore, not much sample material is needed. Some materials under study cannot be easily prepared as large single crystals; polycrystalline arrays may be brittle. Such composites also find applications in which high stiffness or

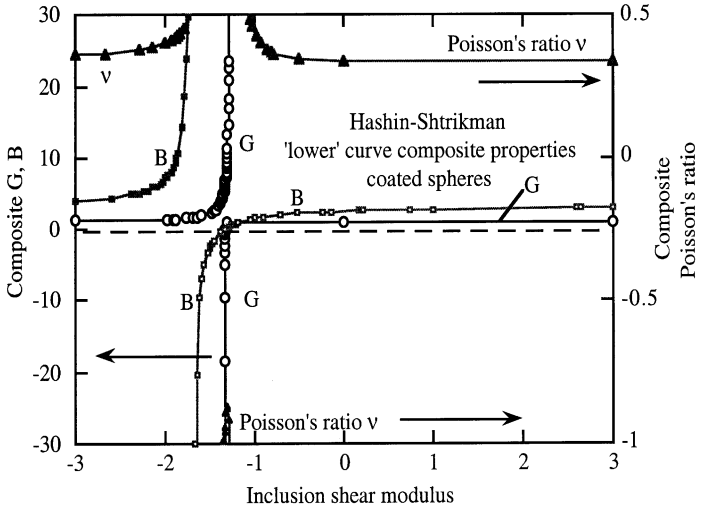

Fig. 10. Isotropic Hashin–Shtrikman 'lower' composite. Composite moduli G and B (normalized to the matrix shear modulus), and composite Poisson's ratio v vs. stiffness of inclusion phase for 5% volume fraction of inclusions. Poisson's ratio $v = 0.1$ for inclusions and 0.35 for matrix.

tunable stiffness is needed. Inclusions need not be temperature-sensitive ferroelastics; pre-stressed or pre-buckled elements may be used as inclusions.

Anomalies (sharp variations) are predicted in composite properties when the inclusions have a negative modulus of magnitude comparable to the matrix modulus. The conclusion is not dependent on the use of extremal composites. The anomalies occur in the following composites: Reuss, Hashin–Shtrikman lower (attainable by hierarchical laminates) and random matrix–inclusion (variational estimate).

The anomalies assume a singular form in composites with linear elastic constituents as well as those with constituents in which the nonlinearity is of a geometrical form. If the matrix has a nonlinearity in the constitutive relation, the anomaly in composite modulus becomes finite. If the constituents are linearly viscoelastic (Lakes, 2001b), then the anomaly in composite modulus is also finite, and is accompanied by a large peak in material damping, $\tan\delta$.

The question of whether one can claim to have considered every possible type of instability that could conceivably occur in composite materials having a negative stiffness phase is obviously a very difficult question that we cannot address fully here. Indeed, it would seem impossible to prove that one had definitively analyzed every possible instability: This is so because we do not believe the question is physically addressable purely within classical elasticity theory. For example, consider the banding instability discussed earlier. It is known from elasticity theory that when strong ellipticity is violated, banding is predicted to be possible from classical elasticity. However, as we noted, experiments have shown that this banding instability is *suppressed* in sufficiently small particles due to the energy penalty of domain formation. Thus, one must incorporate additional physics beyond classical elasticity theory (accompanied by experimental

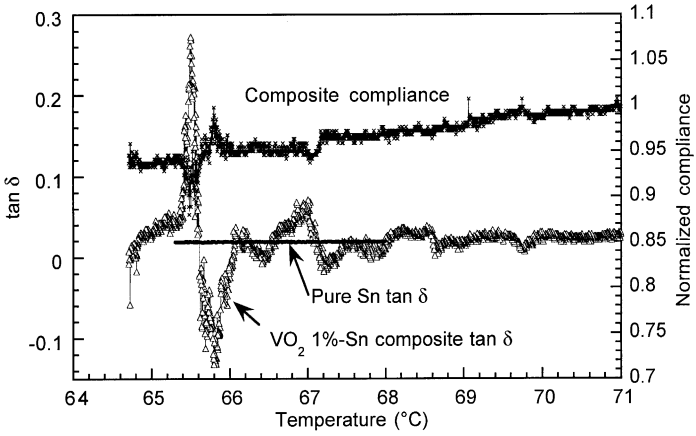

Fig. 11. Experimental torsional compliance and mechanical damping, $\tan\delta$, vs. temperature for a composite containing 1% by volume vanadium dioxide particles in a tin matrix, from Lakes et al. (2001). Measured results for pure tin, for which $\tan\delta = 0.019$ over the temperature range considered, are also plotted for reference. Measurements were conducted at 100 Hz, well below resonance, during slow cooling through the ferroelastic transition of the inclusions.

measurement of the energy penalty, for example) for the theoretical prediction of the permissible regime of this instability to be correct. We anticipate similar scenarios for other instability types.

Further justification that the ideas proposed in this paper are not merely theoretical constructs but have actual real-world merit consists of two sets of experiments performed on viscoelastic materials in which extreme composite material properties (elastic modulus and viscoelastic damping) were actually experimentally attained, and not compromised by unanticipated types of instabilities. The elastic and viscoelastic behavior of composites having a negative stiffness phase has been illustrated for composites with particulate ferroelastic inclusions (Lakes et al., 2001) at 100 Hz, in the quasistatic regime, at least an order of magnitude below the lowest natural frequency, and the viscoelastic behavior for composites with post-buckled tube elements (Lakes, 2001a) at 1 Hz, well below the lowest natural frequency. In the particulate composites, particulate inclusions of vanadium dioxide (VO_2) of 150 μm size or smaller were incorporated into a tin matrix by rolling sheets of tin with particles, followed by casting into a cylindrical mold. Vanadium dioxide is a ferroelastic material which undergoes a transformation from monoclinic to tetragonal at $T_c = 67^\circ$C. Although the concentration of inclusions is dilute, extreme values, well in excess of those of either constituent, were measured in the composite mechanical damping, $\tan\delta$, as well as in the composite stiffness in the vicinity of the transition temperature of the inclusions, as illustrated by the experimental results for a composite with particulate ferroelastic inclusions (Lakes et al., 2001) shown in Fig. 11. Indeed, observed stiffness and damping anomalies in the composite are much larger than they could be for inclusions of any positive stiffness or damping. For example, if the particles were as stiff as diamond ($E = 1000$ GPa), composite theory predicts a composite stiffening effect of only 1.9% and no change in the

viscoelastic damping $\tan\delta$; if the particles were infinitely stiff, the composite would be only 2.1% stiffer than tin matrix. If the particle stiffness were to vanish, the composite would soften by 1.9% and have no change in $\tan\delta$. The inclusions are therefore more effective than diamond in increasing the composite stiffness at selected temperatures; moreover, the composite exceeds the classical bounds based on positive stiffness. The compliance exceeds the Hashin–Shtrikman bounds for this composite (note scale for the compliance on the right in Fig. 11).

In the lumped systems, compliant composite unit cells were made with negative stiffness constituents (Lakes, 2001a). Flexible silicone rubber tubes were incorporated in a post-buckled condition to achieve negative stiffness. Large peaks in mechanical damping $\tan\delta$ of the composite were measured in these systems. Maximum damping was orders of magnitude in excess of the material damping of the silicone rubber.

Acknowledgements

The authors are grateful for a grant, CMS-9896284, from NSF.

Appendix A

A.1. Effective bulk modulus of a composite sphere

To compute the effective bulk modulus of the composite sphere treated in Section 2.3, $\bar{B}$, recall first that this relates the volume-average triaxial stress and strain in the composite as

$$\mathrm{tr}(\bar{\boldsymbol{\sigma}})/3 = \bar{B}\,\mathrm{tr}(\bar{\boldsymbol{\varepsilon}}). \tag{A.1}$$

Also, recall that the volume-average stress and strain are given by

$$\bar{\boldsymbol{\sigma}} \equiv \frac{1}{V}\int_V \boldsymbol{\sigma}\,\mathrm{d}V = \frac{1}{V}\int_S \mathbf{t}\mathbf{x}\,\mathrm{d}S, \quad \bar{\boldsymbol{\varepsilon}} \equiv \frac{1}{V}\int_V \boldsymbol{\varepsilon}\,\mathrm{d}V = \frac{1}{2V}\int_S (\mathbf{n}\mathbf{u} + \mathbf{u}\mathbf{n})\,\mathrm{d}S, \tag{A.2}$$

where $\mathbf{t}$ is the traction vector, $\mathbf{x}$ the position vector, $\mathbf{n}$ the outward unit normal vector to the surface S, $\mathbf{u}$ the displacement vector, and $\mathbf{tx}$, $\mathbf{nu}$ and $\mathbf{un}$ are dyads. For the geometry described in Section 2.3, on the outer boundary of the composite sphere, we have

$$\mathbf{t} = \sigma_{rr}\mathbf{e}_r, \quad \mathbf{x} = b\mathbf{e}_r, \quad \mathbf{n} = \mathbf{e}_r, \quad \mathbf{u} = u_r\mathbf{e}_r, \tag{A.3}$$

where $\mathbf{e}_r$ is the radial unit vector, so that Eq. (A.2) becomes

$$\bar{\boldsymbol{\sigma}} = \sigma_{rr}(b)\mathbf{I}, \quad \bar{\boldsymbol{\varepsilon}} = \frac{u_r(b)}{b}\mathbf{I}, \tag{A.4}$$

where $\mathbf{I}$ is the second-rank identity tensor. Thus, for the present geometry of a sphere containing a spherical inclusion, Eqs. (A.1) and (A.4) with Eqs. (2.2) and (2.4) show that

$$\bar{B} = \frac{\mathrm{tr}(\bar{\boldsymbol{\sigma}})}{3\,\mathrm{tr}(\bar{\boldsymbol{\varepsilon}})} = \frac{b}{3}\,\frac{\sigma_{rr}(b)}{u_r(b)} = \frac{b^3 B_2\alpha_2 - 4G_2\beta_2/3}{\alpha_2 b^3 + \beta_2}. \tag{A.5}$$

As noted by Hill (1963), in this problem the bulk modulus can also be determined from the ratio of the (uniform) applied normal stress to the fractional volume change.

A.2. Finite deformation elasticity solution for spherical symmetry

Here, we show the determination of the finite deformation elasticity solution used in Section 2.3.2; this summarizes and builds on the analysis of Ogden (1984). Since we consider isotropic material, we have that $W(\mathbf{U}) = W(\lambda_1, \lambda_2, \lambda_3)$, where λ_i are the principal stretches, so the principal components of the Biot stress are, from Eq. (2.17),

$$T_i = \frac{\partial W}{\partial \lambda_i}. \tag{A.6}$$

For the spherically symmetric problems to be analyzed, the reference configuration spherical coordinates are R, Θ, Φ, while the current configuration spherical coordinates are r, θ, ϕ. The deformation is thus given by

$$\mathbf{x} = f(R)\mathbf{X} \quad \Rightarrow \quad r = f(R)R, \tag{A.7}$$

where $\mathbf{X}$ and $\mathbf{x}$ are the reference and current configuration position vectors, respectively, and the function $f(R)$ is to be determined. From this, the displacement field is

$$u_R = r - R = [f(R) - 1]R, \tag{A.8}$$

and the deformation gradient tensor is

$$\mathbf{F} = f(R)\mathbf{I} + \frac{1}{R} f'(R)\mathbf{X}\mathbf{X}. \tag{A.9}$$

The spherical symmetry of the deformation demands that $\mathbf{F} = \mathbf{U}$; this with Eq. (A.9) thus shows

$$\lambda_R = Rf'(R) + f(R), \quad \lambda_\Theta = \lambda_\Phi = f(R). \tag{A.10}$$

Thus, for the present spherically symmetric problems, the nonzero components of the right-stretch strain tensor $\mathbf{E} = \mathbf{U} - \mathbf{I}$ are, using Eq. (A.10),

$$E_{RR} = \lambda_R - 1, \quad E_{\Theta\Theta} = E_{\Phi\Phi} = \lambda_\Theta - 1. \tag{A.11}$$

Since $\mathbf{R} = \mathbf{I}$ for the spherically symmetric deformations considered, Eq. (2.16) shows that $\mathbf{S} = \mathbf{T}$, so that the equations of equilibrium $\vec{\nabla} \cdot \mathbf{S} = 0$ take the form

$$\frac{\partial T_{RR}}{\partial R} + \frac{2}{R}(T_{RR} - T_{\Theta\Theta}) = 0, \quad T_{\Theta\Theta} = T_{\Phi\Phi}. \tag{A.12}$$

The stress components appearing in Eq. (A.12) will be the principal stresses of our problems; from Eqs. (2.18) and (A.6), we compute

$$T_{RR} = F'(I_1) - 2c_1\lambda_\Theta + c_2\lambda_\Theta^2, \quad T_{\Theta\Theta} = T_{\Phi\Phi} = F'(I_1) - c_1(\lambda_R + \lambda_\Theta) + c_2\lambda_R\lambda_\Theta. \tag{A.13}$$

Substitution of Eq. (A.13) into Eq. (A.12) leads to

$$\frac{\mathrm{d}}{\mathrm{d}R}[F'(I_1) - c_1 I_1] + c_1\left[\frac{\mathrm{d}\lambda_R}{\mathrm{d}R} + \frac{2}{R}(\lambda_R - \lambda_\Theta)\right] = 0, \tag{A.14}$$

having used Eq. (A.10) and the fact that $I_1 = \lambda_R + 2\lambda_\Theta$; these latter two facts also show that

$$\frac{\mathrm{d}I_1}{\mathrm{d}R} = \frac{\mathrm{d}\lambda_R}{\mathrm{d}R} + \frac{2}{R}(\lambda_R - \lambda_\Theta), \tag{A.15}$$

the use of which reduces Eq. (A.14) to

$$F''(I_1)\frac{\mathrm{d}I_1}{\mathrm{d}R} = 0. \tag{A.16}$$

Since we wish to permit $F''(I_1) \neq 0$ for constitutive flexibility reasons to be discussed shortly, Eq, (A.16) reduces to the requirement

$$\frac{\mathrm{d}I_1}{\mathrm{d}R} \equiv \frac{\mathrm{d}}{\mathrm{d}R}\left(R\frac{\mathrm{d}f}{\mathrm{d}R} + 3f\right) = 0. \tag{A.17}$$

This can be integrated immediately to give the general solution

$$f(R) = 1 + \alpha + \frac{\beta}{R^3}, \tag{A.18}$$

where α and β are as-yet undetermined constants. Thus, from Eqs. (A.8), (A.10) and (A.11), the displacement and strain field solutions will have the forms

$$u_R = \alpha R + \frac{\beta}{R^2}, \tag{A.19}$$

$$E_{RR} = \alpha - 2\frac{\beta}{R^3}, \quad E_{\Theta\Theta} = E_{\Phi\Phi} = \alpha + \frac{\beta}{R^3}. \tag{A.20}$$

We emphasize that the above are the general solutions for arbitrary $F(I_1)$.

As noted in Section 2.3.2, within the finite deformation formulation, we wish to examine both the case of a linear stress–strain constitutive relation and a nonlinear one. Thus, for simplicity we chose $F(I_1)$ to have the specific form:

$$F(I_1) = d_1 I_1^3 + d_2 I_1^2 + d_3 I_1 + d_4 \;\Rightarrow\; F'(I_1) = 3d_1 I_1^2 + 2d_2 I_1 + d_3, \tag{A.21}$$

where $d_1 - d_4$ are constants.

We assume a stress-free reference configuration ($\lambda_R = \lambda_\Theta = \lambda_\Phi = 1$), which from Eq. (A.13) requires

$$F'(3) - 2c_1 + c_2 = 0. \tag{A.22}$$

Applying this requirement to Eq. (A.21) gives

$$27d_1 + 6d_2 + d_3 - 2c_1 + c_2 = 0. \tag{A.23}$$

The spherical symmetry of the composite problems to be analyzed requires equality between two of the principal stretches, $\lambda_\Theta = \lambda_\Phi$, so that for these problems the principal invariants of $\mathbf{U}$ are

$$I_1 = \lambda_R + 2\lambda_\Theta, \quad I_2 = \lambda_\Theta^2 + 2\lambda_R\lambda_\Theta, \quad I_3 = \lambda_R\lambda_\Theta^2. \tag{A.24}$$

Now, for our specific constitutive model Eq. (2.18) with Eq. (2.21), the stress fields Eq. (A.13) become, using Eq. (A.24),

$$T_{RR} = 3d_1(\lambda_R + 2\lambda_\Theta)^2 + 2d_2(\lambda_R + 2\lambda_\Theta) + d_3 - 2c_1\lambda_\Theta + c_2\lambda_\Theta^2,$$

$$T_{\Theta\Theta} = T_{\Phi\Phi} = 3d_1(\lambda_R + 2\lambda_\Theta)^2 + 2d_2(\lambda_R + 2\lambda_\Theta) + d_3 - c_1(\lambda_R + \lambda_\Theta) + c_2\lambda_R\lambda_\Theta. \tag{A.25}$$

By employing Eq. (A.11), these can be written in terms of strain components as, using Eq. (A.23) to substitute for d_3,

$$T_{RR} = 2(9d_1 + d_2)E_{RR} + 2(18d_1 + 2d_2 - c_1 + c_2)E_{\Theta\Theta} + 3d_1E_{RR}^2 + 12d_1E_{RR}E_{\Theta\Theta} + (12d_1 + c_2)E_{\Theta\Theta}^2$$

$$T_{\Theta\Theta} = T_{\Phi\Phi} = (18d_1 + 2d_2 - c_1 + c_2)E_{RR} + (36d_1 + 4d_2 - c_1 + c_2)E_{\Theta\Theta} + 3d_1E_{RR}^2 + (12d_1 + c_2)E_{RR}E_{\Theta\Theta} + 12d_1E_{\Theta\Theta}^2. \tag{A.26}$$

We shall choose the constants in our finite deformation constitutive equation so that Eq. (A.26) reduce to the small-displacement-gradient constitutive equations when strains are infinitesimal:

$$\boldsymbol{\sigma} = 2G\boldsymbol{\varepsilon} + (B - 2G/3)\mathrm{tr}(\boldsymbol{\varepsilon})\mathbf{I}. \tag{A.27}$$

Comparing Eq. (A.26) in the small strain limit with Eq. (A.27) shows that

$$2(9d_1 + d_2) = B + \tfrac{4}{3}G, \quad 18d_1 + 2d_2 - c_1 + c_2 = B - \tfrac{2}{3}G. \tag{A.28}$$

Using Eq. (A.28) to eliminate d_2 and c_1, and for convenience renaming constants as $P \equiv 3d_1$, $Q \equiv c_2$, Eq. (A.26) becomes

$$T_{RR} = (B + \tfrac{4}{3}G)E_{RR} + 2(B - \tfrac{2}{3}G)E_{\Theta\Theta} + P(E_{RR} + 2E_{\Theta\Theta})^2 + QE_{\Theta\Theta}^2,$$

$$T_{\Theta\Theta} = T_{\Phi\Phi} = (B - \tfrac{2}{3}G)E_{RR} + 2(B + \tfrac{1}{3}G)E_{\Theta\Theta} + P(E_{RR} + 2E_{\Theta\Theta})^2 + QE_{RR}E_{\Theta\Theta}. \tag{A.29}$$

References

Balk, A.M., Cherkaev, A.V., Slepyan, L.I., 2001. Dynamics of chains with non-monotone stress–strain relations. I. Model and numerical experiments. J. Mech. Phys. Solids 49, 131–148.

Ball, J.M., 1996. Some recent developments in nonlinear elasticity and its applications to materials science. In: Aston, P.J. (Ed.), Nonlinear Mathematics and its Applications. Cambridge University Press, Cambridge, pp. 93–119.

Bazant, Z., Cedolin, L., 1991. Stability of Structures. Oxford University Press, Oxford.

Berglund, K., 1977. Investigation of a two-dimensional model of a micropolar continuum. Arch. Mech. 29, 383–392.

Cady, W.G., 1964. Piezoelectricity. Dover, New York.

Cosserat, E.F., 1898. Sur les équations de la théorie de l'élasticité. C. R. Acad. Sci. Paris 126, 1089–1091.

Falk, F., 1980. Model free energy, mechanics, and thermodynamics of shape memory alloys. Acta Metall. 28, 1773–1780.

Falk, F., 1983. Ginzburg–Landau theory of static domain walls in shape memory alloys. Z. Phys. B 51, 177–185.

Francfort, G.A., Murat, F., 1986. Homogenization and optimal bounds in linear elasticity. Arch. Rational Mech. Anal. 94, 307–334.

Gibson, L.J., Ashby, M.F., 1988. Cellular Solids. Pergamon, London.

Goodier, J.N., 1933. Concentration of stress around spherical and cylindrical inclusions and flaws. Trans. ASME 55, 39–44 (later called J. Applied Mech., Vol. 1).

Gutierrez, S., 1999. Laminations in linearized elasticity: the isotropic non-very strongly elliptic case. J. Elasticity 53, 215–256.

Hashin, Z., 1962. The elastic moduli of heterogeneous materials. J. Appl. Mech. 29 (Trans. ASME, 84E), 143–150.

Hashin, Z., Shtrikman, S., 1962a. On some variational principles in anisotropic and nonhomogeneous elasticity. J. Mech. Phys. Solids 10, 335–342.

Hashin, Z., Shtrikman, S., 1962b. A variational approach to the theory of the elastic behavior of polycrystals. J. Mech. Phys. Solids 10, 343–352.

Hashin, Z., Shtrikman, S., 1963. A variational approach to the theory of the elastic behavior of multiphase materials. J. Mech. Phys. Solids 11, 127–140.

Hill, R., 1957. On uniqueness and stability in the theory of finite elastic strain. J. Mech. Phys. Solids 5, 229–251.

Hill, R., 1963. Elastic properties of reinforced solids: some theoretical principles. J. Mech. Phys. Solids 11, 357–372.

James, R.D., 1979. Co-existent phases in the one-dimensional static theory of elastic bars. Arch. Rational Mech. Anal. 72, 99–140.

John, F., 1960. Plane strain problems for a perfectly elastic material of harmonic type. Commun. Pure Appl. Math. 13, 239–296.

Lord Kelvin, (Thomson, W.) 1888. On the reflection and refraction of light. Philos. Mag. 26, 414–425.

Knowles, J.K., Sternberg, E., 1978. On the failure of ellipticity and the emergence of discontinuous deformation gradients in plane finite elastostatics. J. Elasticity 8, 329–379.

Lakes, R.S., 1987. Foam structures with a negative Poisson's ratio. Science 235, 1038–1040.

Lakes, R.S., 1991. Deformation mechanisms of negative Poisson's ratio materials: structural aspects. J. Mater. Sci. 26, 2287–2292.

Lakes, R.S., 1993. Advances in negative Poisson's ratio materials. Adv. Mater. 5, 293–296.

Lakes, R.S., 2001a. Extreme damping in compliant composites with a negative stiffness phase. Philos. Mag. Lett. 81, 95–100.

Lakes, R.S., 2001b. Extreme damping in composite materials with a negative stiffness phase. Phys. Rev. Lett. 86, 2897–2900.

Lakes, R.S., Lee, T., Bersie, A., Wang, Y.C., 2001. Extreme damping in composite materials with negative stiffness inclusions. Nature 410, 565–567.

Lines, M.E., Glass, A.M., 1979. Principles and Applications of Ferroelectrics and Related Materials. Clarendon Press, Oxford.

Love, A.E.H., 1944. A Treatise on the Mathematical Theory of Elasticity. Dover, New York.

Milton, G.W., 1986. Modeling the properties of composites by laminates. In: Erickson, J.L., Kinderlehrer, D., Kohn, R., Lions, J.L. (Eds.), Homogenization and Effective Moduli of Materials and Media. Springer, Berlin, pp. 150–175.

Milton, G.W., 2001. Theory of Composites. Cambridge University Press, Cambridge.

Milton, G.W., Serkov, S.K., 2001. Neutral coated inclusions in conductivity and anti-plane elasticity. Proc. Roy. Soc. 457, 1973–1997.

Nicorovici, N.A., Mcphedran, R.C., Milton, G.W., 1994. Optical and dielectric properties of partially resonant systems. Phys. Rev. B 49, 8479–8482.

Ogden, R.W., 1984. Non-Linear Elastic Deformations. Ellis Harwood Ltd, Chichester, UK (1997, Dover, New York).

Paul, B., 1960. Prediction of elastic constants of multiphase materials. Trans. AIME 218, 36–41.

Puglisi, G., Truskinovsky, L., 2000. Mechanics of a discrete chain with bi-stable elements. J. Mech. Phys. Solids 48, 1–27.

Rosakis, P., Ruina, A., Lakes, R.S., 1993. Microbuckling instability in elastomeric cellular solids. J. Mater. Sci. 28, 4667–4672.

Salje, E., 1990. Phase Transitions in Ferroelastic and Co-elastic Crystals. Cambridge University Press, Cambridge.

Timoshenko, S.P., Goodier, J.N., 1970. Theory of Elasticity, 3rd Edition. McGraw-Hill, New York.

Timoshenko, S.P., 1983. History of Strength of Materials. Dover, New York.

Truesdell, C., Noll, W., 1965. The non-linear field theories of mechanics. In: Flugge, S. (Ed.), Handbuch der Physik, Vol. III. Springer, Berlin.

Willis, J.R., 1977. Bounds and self-consistent estimates for the overall properties of anisotropic composites. J. Mech. Phys. Solids 25, 185–202.

Willis, J.R., 1982. Elasticity theory of composites. In: Hopkins, H.G., Sewell, M.J. (Eds.), Mechanics of Solids: The R. Hill 60th Anniversary Volume. Pergamon Press, Oxford, pp. 653–686.